

Article

# Radiation Dose to Critical Cardiac Structures from Three-Dimensional Conformal Radiation Therapy (3D-CRT), Intensity-Modulated Radiation Therapy (IMRT) and Volumetric Modulated Arc Therapy (VMAT) Techniques for Left-Sided Breast Cancer

Evgenia Konstantinou <sup>1</sup>, Antonis Varveris <sup>2</sup> , Georgia Solomou <sup>3</sup>, Chrysostomos Antoniadis <sup>2</sup>, Maria Tolia <sup>2</sup>  and Michalis Mazonakis <sup>1,\*</sup>

<sup>1</sup> Department of Medical Physics, Faculty of Medicine, University of Crete, 71003 Heraklion, Greece

<sup>2</sup> Department of Radiotherapy and Oncology, University General Hospital of Heraklion, 71110 Heraklion, Greece

<sup>3</sup> Department of Medical Physics, University General Hospital of Heraklion, 71110 Heraklion, Greece

\* Correspondence: mazonak@uoc.gr; Tel.: +30-2810392342



**Citation:** Konstantinou, E.; Varveris, A.; Solomou, G.; Antoniadis, C.; Tolia, M.; Mazonakis, M. Radiation Dose to Critical Cardiac Structures from Three-Dimensional Conformal Radiation Therapy (3D-CRT), Intensity-Modulated Radiation Therapy (IMRT) and Volumetric Modulated Arc Therapy (VMAT) Techniques for Left-Sided Breast Cancer. *J. Pers. Med.* **2024**, *14*, 63. <https://doi.org/10.3390/jpm14010063>

Academic Editor: Yong Wu

Received: 24 November 2023

Revised: 29 December 2023

Accepted: 30 December 2023

Published: 3 January 2024



**Copyright:** © 2024 by the authors. Licensee MDPI, Basel, Switzerland. This article is an open access article distributed under the terms and conditions of the Creative Commons Attribution (CC BY) license (<https://creativecommons.org/licenses/by/4.0/>).

**Abstract:** A comparison of the radiation exposure to the left anterior descending artery (LAD) and left ventricle (LV) was performed for twenty-three left breast cancer patients. For each participant, two tangential fields 3D-CRT, two- and seven-field IMRT and two and four partial arcs VMAT plans were created. Dose constraints for CTV, ipsilateral lung and heart were followed. The  $V_{40Gy}$ ,  $V_{30Gy}$ ,  $D_{av}$  of LAD and  $V_{23Gy}$ ,  $V_{5Gy}$ ,  $D_{av}$  of LV were calculated and extracted from the plans. Parametric and non-parametric tests were applied to compare the parameters derived from the five treatment techniques. All generated plans fulfilled the dose constraints. The  $D_{av}$  ranges of the LAD and LV from all examined techniques were 11.77–14.73 Gy and 5.37–6.40 Gy, respectively. The  $V_{40Gy}$  and  $V_{30Gy}$  ranges of the LAD were 2.90–12.91% and 10.80–18.51%, respectively. The  $V_{23Gy}$  and  $V_{5Gy}$  of the LV were 4.29–7.43% and 18.24–30.05%, respectively. The VMAT plans and seven-field IMRT significantly reduced the  $V_{40Gy}$ ,  $V_{30Gy}$  of LAD and  $V_{23Gy}$  of LV compared with the two-field treatments ( $p < 0.05$ ). However, 3D-CRT plans provided statistically lower values for  $V_{5Gy}$  of LV over the other techniques ( $p < 0.05$ ). The presented results provide a detailed dataset of the radiation burden of two critical cardiac structures from five radiotherapy techniques.

**Keywords:** left breast cancer; LAD; LV; 3D-CRT; IMRT; VMAT

## 1. Introduction

Female breast cancer is the most frequently diagnosed cancer and the fifth leading cause of cancer death worldwide [1]. According to global statistics in 2020 [1], over 2.2 million breast cancer incidents were recorded, accounting for approximately 700 thousand deaths. An improved 5-year survival rate of 90.8% has been reported for females diagnosed with breast malignancies between 2013 and 2018 in USA [2]. This has been attributed to early cancer detection through mammographic screening and to advances in applied anticancer treatment [3,4].

Whole breast radiation therapy (WBRT) after breast-conserving surgery (BCS) is indicated for early-stage breast cancer patients [5]. The adjuvant radiotherapy enhances the reduction of local recurrence as well as the risk of breast cancer death [6,7]. However, radiotherapy may induce cardiac toxicity [8–10]. Darby et al. [8] found that the relative risk for developing major coronary events in females irradiated for breast cancer is 7.4% per Gy received by the whole heart without apparent threshold for breast cancer patients who received radiotherapy. After the exposure, the risk started rising within the first five years

and continued for more than 20 years. Left-sided breast cancer patients are at an increased risk of developing heart diseases compared with right-sided patients [9–11]. Moreover, higher rates of cardiac death were observed for these patients [9,12,13]. Bouillon et al. [13] showed that patients who were irradiated for left breast cancer had a 1.56-fold greater risk of cardiac disease death than patients treated for right breast malignancies.

Radiation-induced cardiotoxicity is associated with the exposure of the heart and its substructures, mainly the left anterior descending artery (LAD) and the left ventricle (LV). The LAD artery, which is located at the anterior part of the heart, receives significant radiation dose due to radiotherapy [14–16]. Irradiating the LAD artery can cause coronary artery disease which then results in subsequent ischemic disease [8,11,14]. Complications in the left ventricle related to radiotherapy such as perfusion defects and segmental alterations have previously been recorded [17–19]. Subclinical LV dysfunction appeared 6 months after the radiotherapy, as reported by Walker et al. [18]. Recent studies [20,21] have proved that the deep inspiration breath-hold technique effectively contributes to a dose-sparing effect on the heart and these two cardiac substructures compared with free breath. However, this technique is not widely applicable at present.

Breast cancer irradiation may be based on the conventional three-dimensional conformal radiotherapy (3D-CRT) [22]. More advanced techniques such as intensity-modulated radiation therapy (IMRT) and volumetric modulated arc therapy (VMAT) may also be applied for the management of this malignancy [22]. Limited information exists in the literature about the comparison of the above three treatment techniques in respect to the radiation exposure of LAD and LV. Kuzba-Kryszak et al. [23] provided data about the dose to LAD from 3D-CRT, IMRT and VMAT. Their investigation was carried out for the deep inspiration breath-hold technique. No information was given about the LV. To our knowledge, no attempt has been conducted to directly compare the three radiotherapy techniques in free breathing conditions.

The objective of this study was to compare the dosimetric parameters of the LAD and LV from 3D-CRT, IMRT with two and seven fields and VMAT with two and four partial arcs for left breast cancer patients.

## 2. Materials and Methods

### 2.1. Patients

Twenty-three left-sided breast cancer patients who had previously undergone radiotherapy at the Radiation Oncology department of the University General Hospital of Heraklion were included in this study. The treatment of all patients had been completed prior to the beginning of this work. Whole breast irradiation was performed. For the implementation of this study, approval was granted by the Ethics Committee at the University General Hospital of Heraklion. All study participants were diagnosed with early stage left breast cancer (T1–T2). The patients' tumor grade was 1–3. These patients had undergone breast-conserving surgery followed by adjuvant whole breast irradiation. Patients with metastatic disease were excluded. Moreover, patients needing axillary or lymph node irradiation were not included in the patient group of this work. The patients' mean age was  $55 \pm 12$  years old (range: 31–83); 61% of the total number of patients were under the mean patient age of 55 years old.

### 2.2. Planning Computed Tomography

In supine position, patients were immobilized with both arms upward on a breast board and the head facing to the right. Planning images were acquired using a 16-slice computed tomography unit (Somatom Sensation 16, Siemens, Forchheim, Germany). The clinical target volume (CTV) ranged between  $237 \text{ cm}^3$  and  $2535 \text{ cm}^3$ , with a mean value of  $918 \pm 506 \text{ cm}^3$ . The planning target volume (PTV) was generated by adding a 3 mm margin around the CTV. The heart and the ipsilateral lung were determined as the organs at risk. The process of contouring on the computed tomography images was based on previously published guidelines of the European Society for Therapeutic Radiology and Oncology [24]. The contouring of the target volume and all the involved surrounding organs were carried out

with the aid of the treatment planning system (Monaco 5.11, Elekta AB, Stockholm, Sweden). Manual delineation on computed tomography scans was performed by a radiation oncologist experienced in breast cancer treatment. In addition, the same radiation oncologist contoured the two cardiac structures, the LAD and LV. A senior radiation oncologist consistently carried out a review of the contours of all structures on a slice-by-slice basis and performed the necessary changes and corrections. The LAD artery and the LV as well as their ramifications were manually delineated on a slice-by-slice basis in accordance with previously reported data [25,26]. Figure 1 shows all the contoured structures.

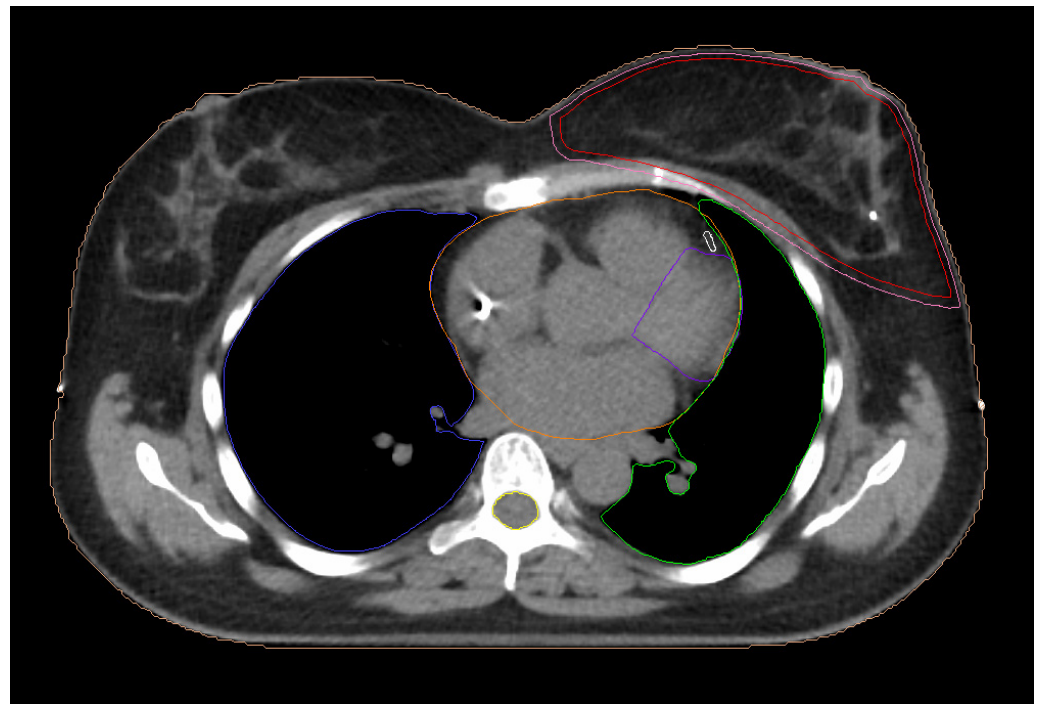


**Figure 1.** Computed tomography image with contoured structures: CTV (red); PTV (pink); heart (orange); ipsilateral lung (green); contralateral lung (blue); LAD (white); left ventricle (purple); spinal cord (yellow).

### 2.3. Treatment Planning

Treatment planning was made using the Monaco system for beam delivery on an Infinity linear accelerator (Elekta AB, Stockholm, Sweden). The treatment plans were generated with 6 MV photons which is the standard currently employed in our department for all breast cancer patients. The above photon energy is usually preferred for breast cancer management to avoid the underdose of superficial tissues beneath the skin surface [27]. The isocenter was placed in the center of the PTV. Radiotherapy treatment plans were made with five different techniques for each patient. The treatment techniques examined in this work have already been employed in previously published studies [23,28,29]. The radiation dose to the LV and LAD artery was not considered in the optimization process during treatment planning.

The prescription dose for CTV was 50 Gy given in 25 fractions of 2 Gy. The dose constraints for the target volume and the critical organs were based on the Danish Breast Cancer Group Hypo trial [30] for whole breast radiation therapy. In this model, 95% of the CTV had to received 95% of the total dose ( $D_{95\%} \geq 47.5$  Gy), while the maximum dose should not be greater than 55 Gy. The volume of ipsilateral lung receiving a dose of 20 Gy had to be kept less than 20% ( $V_{20Gy} < 20\%$ ). The heart's constraints were  $V_{20Gy} < 10\%$  and  $V_{40Gy} < 5\%$ . Additionally, through the treatment planning system we recorded other dosimetric parameters which are shown in Table 1. The LAD and LV parameters were based on the recommendations of Piroth et al. [31] as representative for heart protection from high therapeutic doses. They defined the dosimetric parameters of both cardiac structures on the basis of the clinical evidence on cardiac toxicities owing to radiation [31].

The same dosimetric parameters for the LAD and LV structures have previously been used in studies dealing with radiotherapy for breast carcinomas [32–34].

**Table 1.** Dosimetric parameters of planning target volume (PTV), heart and cardiac structures.

Structure	Dosimetric Parameters
PTV	$D_{95\%}$
Heart	$D_{av}$
LAD	$V_{40Gy}$ $V_{30Gy}$ $D_{av}$
LV	$V_{23Gy}$ $V_{5Gy}$ $D_{av}$

$D_{95\%}$ : target percentage receiving 95% of total dose;  $D_{av}$ : average dose;  $V_{iGy}$ : organ volume receiving less than iGy.

### 2.3.1. 3D-CRT Technique

All plans with 3D conformal radiation therapy consisted of two tangential fields without wedges (Figure 2a). Gantry's angle for the internal field ranged from  $300^\circ$  to  $315^\circ$ , while for the external field it was between  $123^\circ$  and  $140^\circ$ . The beams' angles were selected on the basis of a beam-eye-view approach. The directions and weights of the applied beams were chosen to optimize the coverage of CTV and to restrict the radiation dose received by the surrounding organs. Furthermore, an expansion was added in both PTV and anteriorly from the chest wall to create the “flash” region. To avoid hot spots and creating homogeneous dose distribution we generated low weight segments using multileaf collimator. The number of segments varied among patients. No more than four segments were added per treatment field. Plans were designed by a forward planning system using a collapsed cone algorithm.

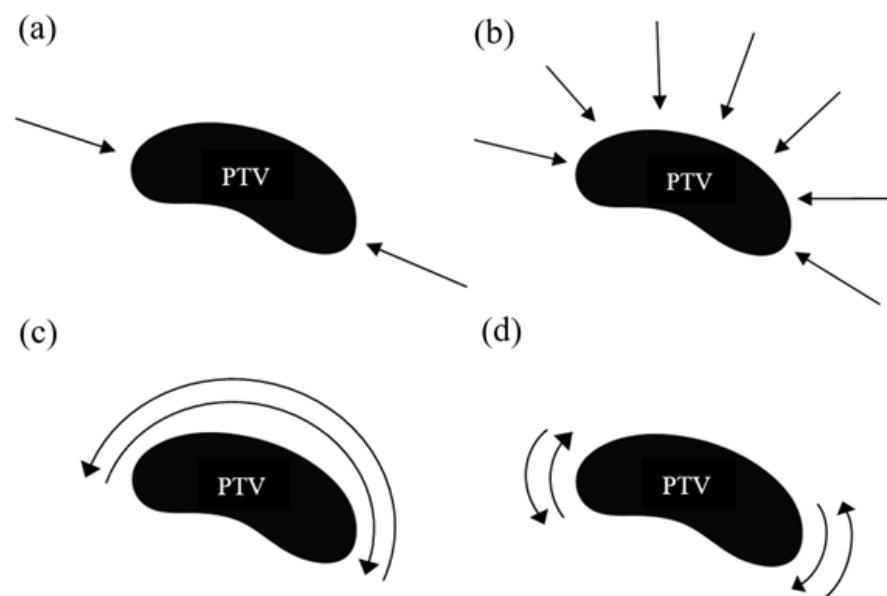


**Figure 2.** Beam and arc arrangements for the planning techniques: (a) 3D-CRT and two-fields IMRT (2F-IMRT); (b) seven-fields IMRT (7F-IMRT); (c) two partial arcs VMAT (VMAT1); (d) four partial arcs VMAT (VMAT2).

### 2.3.2. Two-Field IMRT Technique (2F-IMRT)

The plans for this technique were implemented with two opposed fields (Figure 2a). For each individual, the field angles were the same as the 3D-CRT technique. In this context, in

seven patients an additional field was added to improve higher coverage in CTV with an angle of  $340^\circ$  or  $345^\circ$ . Inverse planning was performed with dynamic multileaf collimator delivery. The maximum number of control points was 20 per beam. Dose calculation was carried out with a Monte Carlo algorithm and then it was optimized with the fluence optimizer algorithm using a 0.5 cm grid. The collimator was angled to adjust the chest wall shape.

### 2.3.3. Seven-Field IMRT Technique (7F-IMRT)

Multibeam IMRT comprised seven coplanar beams. The beams were equally spaced through a sector angle of  $190^\circ$  around the target volume [5]. For each beam, the control points were up to 20. A typical beam arrangement is illustrated in Figure 2b.

### 2.3.4. Two Partial-Arc VMAT Technique (VMAT1)

A VMAT plan consisting of a dual partial arc was applied for all participants. The length of each arc was always  $200^\circ$ . The starting angle ranged between  $293^\circ$  and  $306^\circ$ . The two coplanar arcs rotated in clockwise and counterclockwise directions. This dual arc approach is widely applied for VMAT planning [35–37]. Figure 2c presents the positioning of partial arcs. VMAT plans were created by using a 0.5 cm grid and the maximum number of control points was 150. For all plans, the collimator was in  $0^\circ$ .

### 2.3.5. Four Partial-Arc VMAT Technique (VMAT2)

Two double partial arcs of  $50^\circ$  each were used in VMAT plans (Figure 2d). Each double arc comprised of a counterclockwise and a clockwise arc. For the internal arc, the irradiation starting point varied from  $283^\circ$  to  $295^\circ$ , while the external arc was  $103^\circ$  to  $120^\circ$ . All treatment plans were designed inversely using a 0.5 cm grid. The maximum number of control points was 100 for each arc and the collimator was in  $0^\circ$ . The gantry rotated both clockwise and anticlockwise. The dual arc approach is currently employed in our department for the creation of all VMAT plans [5].

## 2.4. Statistical Analysis

Statistical analysis was performed using the Statistical Package for the Social Sciences (SPSS) for Windows version 28.0 (IMB Corp., Armonk, NY, USA). The mean and standard deviation were calculated for all the dosimetric parameters of all contoured structures. Further analysis was conducted for the LAD and LV. The differences in the  $V_{40Gy}$ ,  $V_{30Gy}$  and  $D_{av}$  of the LAD as calculated for the five treatment planning strategies were evaluated. The above process was carried out for the parameters related to LV. Statistical tests have been successfully used to indicate significant differences between dosimetric and/or radiobiological parameters determined by different radiation therapy techniques [38]. Normalization analysis was carried out with the Shapiro–Wilk test for all the variables. Subsequently, the paired sample *t*-test and the Wilcoxon signed ranks test were used for variables comparison of treatment plans. A significance level of 5% was determined.

## 3. Results

### 3.1. Treatment Evaluation

All treatment plans fulfilled the dose constraints, and they were considered clinically acceptable. VMAT1 and VMAT2 plans are presented in Figure 3 with isodoses covering the target volume. Table 2 summarizes the mean values of the planning parameters for the CTV, PTV and the surrounding organs. The 7F-IMRT, VMAT2, VMAT1 techniques led to mean  $D_{95\%}$  of 99.12%, 99.00%, 98.86%, respectively. The 2F-IMRT and 3D-CRT plans gave lower values of 97.04% and 96.56% accordingly. Similar results were found for the  $D_{95\%}$  of the PTV. The highest dose coverage for PTV of 96.45% was achieved for VMAT2 followed by 7F-IMRT and VMAT1 with mean values of more than 95.46%. The mean  $V_{40Gy}$  of the heart associated with the two VMAT techniques and 7F-IMRT varied from 0.52 to 0.67% whereas the range for  $V_{20Gy}$  was 3.17 to 3.38%. The  $V_{40Gy}$  and  $V_{20Gy}$  from techniques comprising only two tangential treatment fields were at least 1.65% and 4.65%. The  $D_{av}$  of



the heart from the conventional 3D-CRT was 3.70 Gy. The IMRT and VMAT techniques led to  $D_{av}$  of 5.15 Gy or more. The 7F-IMRT, VMAT1 and VMAT2 plans provided a mean  $V_{20Gy}$  of the ipsilateral lung of 8.90%, 9.65% and 10.00%, respectively. The corresponding value from both 3D-CRT and 2F-IMRT was more than 11.22%.

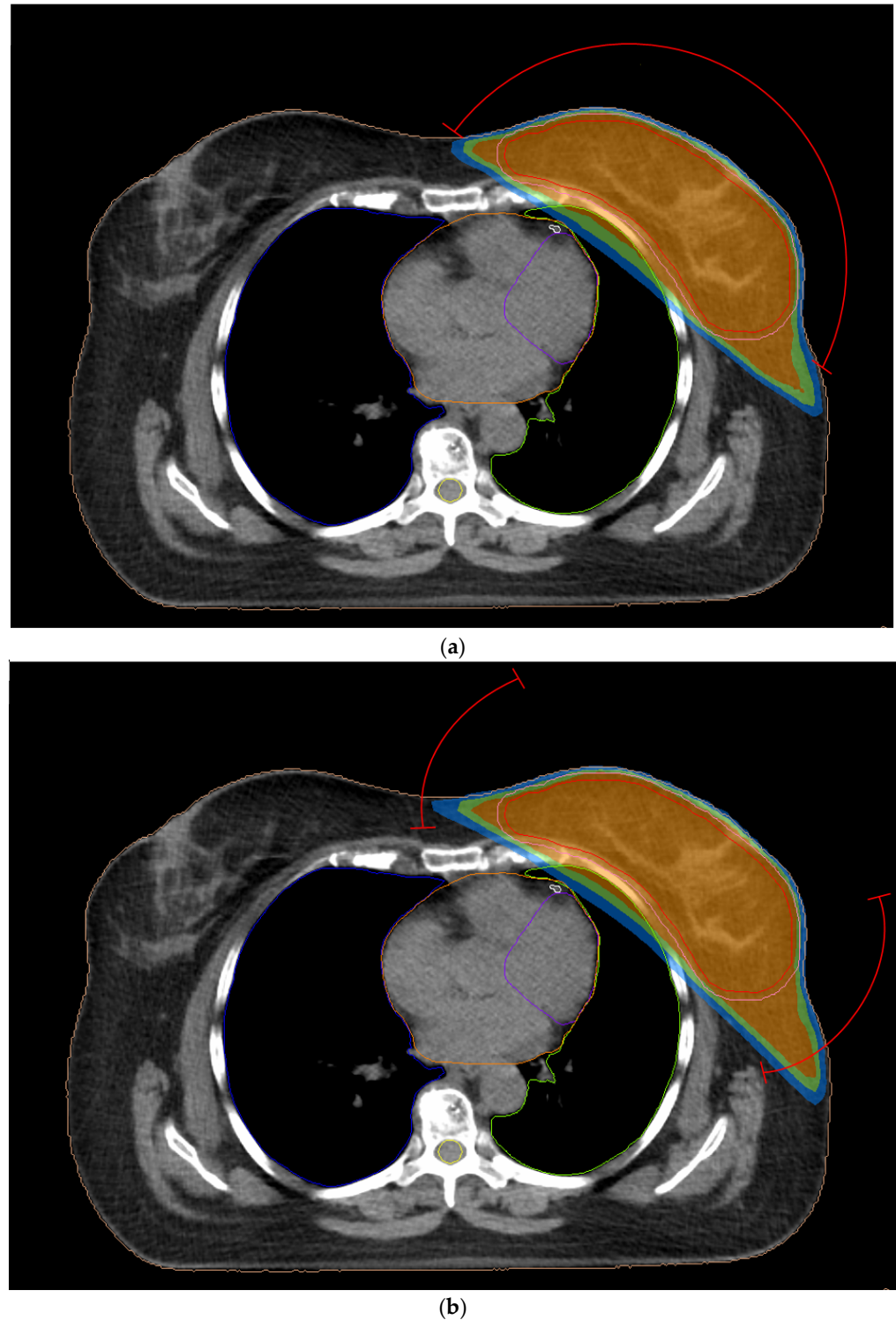


**Figure 3.** Computed tomography image with contoured structures: CTV (red); PTV (pink); heart (orange); ipsilateral lung (green); contralateral lung (blue); LAD (white); left ventricle (purple); spinal cord (yellow). Treatment plans of left breast cancer with dose distribution around the target volume (red) which treated with (a) two partial-arc VMAT and (b) four partial-arc VMAT. The isodoses of orange, green and blue color correspond to 95%, 85% and 70% of total dose, respectively.

**Table 2.** Dosimetric parameters for CTV, PTV, whole heart and ipsilateral lung as derived from five different treatment planning techniques. Dose values are given as mean  $\pm$  one standard deviation.

Structure	Parameter	Mean $\pm$ Standard Deviation				
		3D-CRT	2F-IMRT	7F-IMRT	VMAT1	VMAT2
CTV	D <sub>95%</sub> (%)	96.56 $\pm$ 1.45	97.04 $\pm$ 1.73	99.12 $\pm$ 1.00	98.86 $\pm$ 1.30	99.00 $\pm$ 1.13
PTV	D <sub>95%</sub> (%)	92.11 $\pm$ 1.95	92.68 $\pm$ 1.62	96.04 $\pm$ 0.98	95.46 $\pm$ 1.09	96.45 $\pm$ 1.30
Heart	V <sub>40Gy</sub> (%)	1.88 $\pm$ 1.31	1.65 $\pm$ 1.34	0.67 $\pm$ 0.68	0.55 $\pm$ 0.56	0.52 $\pm$ 0.58
	V <sub>20Gy</sub> (%)	4.65 $\pm$ 2.19	4.67 $\pm$ 2.37	3.38 $\pm$ 1.72	3.28 $\pm$ 1.94	3.17 $\pm$ 1.82
	D <sub>av</sub> (Gy)	3.70 $\pm$ 0.98	6.43 $\pm$ 10.60	5.21 $\pm$ 1.04	5.15 $\pm$ 1.08	5.99 $\pm$ 9.54
Isp. lung	V <sub>20Gy</sub> (%)	11.40 $\pm$ 4.76	11.22 $\pm$ 4.51	8.90 $\pm$ 3.26	9.65 $\pm$ 3.36	10.00 $\pm$ 3.47

CTV: clinical target volume; PTV: planning target volume; 3D-CRT: three-dimensional conformal radiotherapy; 2F: two fields; 7F: seven fields; IMRT: intensity-modulated radiation therapy; VMAT: volumetric modulated arc therapy; VMAT1: VMAT with two partial arcs; VMAT2: VMAT with four partial arcs.

### 3.2. Exposure of Cardiac Structures

The calculated mean value and standard deviation of LAD and LV dosimetric parameters are summarized in Table 3. For both critical structures, the differences between the parameters derived from the five examined techniques are presented in Table 4.

**Table 3.** Dosimetric parameters for LAD and LV as derived from five different treatment planning techniques. Dose values are given as mean  $\pm$  one standard deviation.

Structure	Parameter	Mean $\pm$ Standard Deviation				
		3D-CRT	2F-IMRT	7F-IMRT	VMAT1	VMAT2
LAD	V <sub>40Gy</sub> (%)	12.91 $\pm$ 11.76	10.30 $\pm$ 10.74	4.98 $\pm$ 8.04	2.90 $\pm$ 5.91	3.10 $\pm$ 6.08
	V <sub>30Gy</sub> (%)	18.51 $\pm$ 13.00	17.48 $\pm$ 13.73	12.84 $\pm$ 11.96	10.80 $\pm$ 10.84	10.88 $\pm$ 12.07
	D <sub>av</sub> (Gy)	12.94 $\pm$ 5.33	14.73 $\pm$ 9.40	12.92 $\pm$ 5.51	12.02 $\pm$ 4.91	11.77 $\pm$ 5.05
LV	V <sub>23Gy</sub> (%)	7.43 $\pm$ 4.18	7.26 $\pm$ 4.50	4.53 $\pm$ 3.27	4.47 $\pm$ 3.36	4.29 $\pm$ 3.40
	V <sub>5Gy</sub> (%)	18.24 $\pm$ 6.26	28.77 $\pm$ 17.46	30.05 $\pm$ 14.38	29.99 $\pm$ 14.75	25.80 $\pm$ 14.05
	D <sub>av</sub> (Gy)	5.69 $\pm$ 1.92	6.40 $\pm$ 1.75	5.93 $\pm$ 1.77	5.89 $\pm$ 1.80	5.37 $\pm$ 1.76

LAD: left anterior descending; LV: left ventricle; 3D-CRT: three-dimensional conformal radiotherapy; 2F: two fields; 7F: seven fields; IMRT: intensity-modulated radiation therapy; VMAT: volumetric modulated arc therapy; VMAT1: VMAT with two partial arcs; VMAT2: VMAT with four partial arcs.

**Table 4.** Statistical comparison between the five different treatment planning techniques for the dosimetric parameters of the LAD and LV.

Techniques Comparison	<i>p</i> -Value					
	LAD			LV		
	V <sub>40Gy</sub>	V <sub>30Gy</sub>	D <sub>av</sub>	V <sub>23Gy</sub>	V <sub>5Gy</sub>	D <sub>av</sub>
3D-CRT vs. 2F-IMRT	0.007 *	0.101	0.316	0.546	<0.001 *	0.007 *
3D-CRT vs. 7F-IMRT	<0.001 *	<0.001 *	0.967	<0.001 *	<0.001 *	0.277
3D-CRT vs. VMAT1	<0.001 *	<0.001 *	0.125	<0.001 *	<0.001 *	0.412
3D-CRT vs. VMAT2	<0.001 *	<0.001 *	0.016 *	<0.001 *	0.002 *	0.110
2F-IMRT vs. 7F-IMRT	<0.001 *	<0.001 *	0.484	<0.001 *	0.162	0.144
2F-IMRT vs. VMAT1	<0.001 *	<0.001 *	0.039 *	<0.001 *	0.144	0.124
2F-IMRT vs. VMAT2	<0.001 *	<0.001 *	0.008 *	<0.001 *	0.533	0.002 *
7F-IMRT vs. VMAT1	0.039 *	0.071	0.014 *	0.436	0.966	0.809
7F-IMRT vs. VMAT2	0.019 *	0.198	0.008 *	0.263	0.104	0.002 *
VMAT1 vs. VMAT2	0.767	0.629	0.545	0.487	0.098	0.002 *

LAD: left anterior descending; LV: left ventricle; 3D-CRT: three-dimensional conformal radiotherapy; 2F: two fields; 7F: seven fields; IMRT: intensity-modulated radiation therapy; VMAT: volumetric modulated arc therapy; VMAT1: VMAT with two partial arcs; VMAT2: VMAT with four partial arcs. \* Statistically significant differences ( $p < 0.05$ ).

### 3.2.1. Left Anterior Descending Artery (LAD)

The 7F-IMRT and two VMAT techniques led to mean  $V_{40Gy}$  and  $V_{30Gy}$  values of 2.90–4.98% and 10.80–12.84%, respectively. For the techniques that consisted of two fields, the  $V_{40Gy}$  and  $V_{30Gy}$  were no less than 10.30% and 17.48%. Significant statistical differences were observed between the LAD parameters obtained by IMRT, VMAT1 and VMAT2 plans from these calculated by two-field treatments (Table 4). In addition, VMAT1 plans provided a statistically lower value for  $V_{40Gy}$  compared with 7F-IMRT plans (2.90% vs. 4.98%,  $p = 0.039$ ). The range of mean  $D_{av}$  was 11.77–14.73 Gy, using the five irradiation approaches. Statistical difference was found by comparing VMAT2 plans with 3D-CRT, 2F-IMRT and 7F-IMRT. This was also found between VMAT1 and 2F-IMRT and 7F-IMRT ( $p = 0.039$ ; 0.014 respectively).

### 3.2.2. Left Ventricle (LV)

Assessing the mean  $V_{23Gy}$  of the LV, the lowest mean values were derived from VMAT2, VMAT1 and 7F-IMRT plans at 4.29%, 4.47% and 4.53%, respectively. The 2F-IMRT and 3D-CRT plans gave mean values of 7.26% and 7.43%. According to Table 4, significant difference was observed for 7F-IMRT, VMAT1 and VMAT2 plans ( $p < 0.001$ ) over the 3D-CRT and 2F-IMRT. The mean  $V_{5Gy}$  was 18.24% for conformal treatment and was increased from 25.80 to 30.05% with the use of other techniques. Statistical difference was exhibited when comparing 3D-CRT with the other four techniques (Table 4). Among the five examined techniques, the  $D_{av}$  varied between 5.37 Gy and 6.40 Gy. There was a significant difference between VMAT2 plans with 2F-IMRT, 7F-IMRT and VMAT1 plans ( $p = 0.002$ ) and 3D-CRT with 2F-IMRT ( $p = 0.007$ ).

## 4. Discussion

The high doses received by the LAD and LV structures after radiotherapy for left breast cancer may increase the risk of heart complications despite the low mean heart dose. This study examined the radiation exposure of both LAD and LV from radiotherapy for left breast cancer patients. Five different treatment techniques were applied including the 3D-CRT, IMRT with two and seven fields and VMAT with two and four partial arcs. For all the generated plans, we did not apply any optimization objective for the LAD and LV structures.

The treatment plans of all study participants satisfied the dose constraints, and they were considered as acceptable for clinical use. For seven patients, a third field was added in the 2F-IMRT plans to increase the dose coverage in the CTV. The two VMAT techniques and 7F-IMRT provided superior target volume coverage as well as leading to lower mean values for  $V_{20Gy}$  of left lung and  $V_{40Gy}$ ,  $V_{20Gy}$  of heart. In addition, 7F-IMRT, VMAT1 and VMAT2 plans significantly contributed to the LAD artery dose sparing when evaluating the  $V_{40Gy}$  and  $V_{30Gy}$ . A superiority of VMAT1 plans instead of 7F-IMRT in respect to  $V_{40Gy}$  was found. For the  $V_{23Gy}$  of the LV, a statistically significant dose reduction was observed with the use of the 7F-IMRT and VMAT planning methods over the two tangential techniques. On the other hand, the 3D-CRT technique resulted in significantly lower  $V_{5Gy}$  as opposed to other techniques. Furthermore, it is noteworthy to mention that the  $D_{av}$  received by the LAD was substantially higher than the  $D_{av}$  of the whole heart (Tables 2 and 3). Similar results were found, though with less variation, for the LV.

Kuzba-Kryszak et al. [23] compared the 3D-CRT, IMRT and VMAT planning techniques in deep inspiration breath-hold conditions. They reported a  $D_{av}$  for the LAD of 19.72 Gy, 13.00 Gy and 19.13 Gy for the above techniques, respectively. A slight dose reduction in the LAD artery was observed by applying inverse planning techniques. However, direct comparison with our study cannot be made because their investigation was carried out in patients receiving breath-hold radiotherapy to 42.5 Gy with 6 and 15 MV beams. Another study was conducted by Zhang et al. [39]. They estimated LV exposure with the use of 3D-CRT and two IMRT techniques. All IMRT plans included six beams, while the second IMRT used a lower number of segments with greater minimum area. Our results related



to the  $D_{av}$  of the LV from 3D-CRT and 7F-IMRT plans were lower than their results. The  $D_{av}$  of the LV in their study was 12.54 Gy, 15.56 Gy and 16.37 Gy for two tangential fields 3D-CRT and the two IMRT plans respectively. In addition, their 3D-CRT plans provided significantly lower  $D_{av}$  and  $V_{5Gy}$  compared with the IMRT plans. However, no significant difference was found between the two IMRT plans and 3D-CRT for the high-dose volume parameter ( $V_{25Gy}$ ). Regarding our results, statistical difference between 7F-IMRT and 3D-CRT was observed for  $V_{23Gy}$  and  $V_{5Gy}$ . Moreover, Karpf et al. [40] showed that multibeam step-and-shoot IMRT plans significantly reduced the  $D_{av}$  of the LAD when compared with four semi-arc VMAT plans (5.80 Gy vs. 7.32 Gy,  $p = 0.03$ ). In our study, the 7F-IMRT led to a significantly higher  $D_{av}$  of the LAD compared with the VMAT plans.

Regarding our findings, the examined dosimetric parameters of the two cardiac structures were higher than the values recommended by Piroth et al. [31]. This was not observed for  $V_{23Gy}$  of the LV for the 7F-IMRT, VMAT1 and VMAT2 plans. The planning results of this study were extracted without considering the radiation dose for the LAD and LV in the optimization process. This indicates that the treatment plans should be evaluated and for the heart substructures beyond the whole heart.

The current study may be limited by the relatively small size of left-sided breast cancer patients. All participants received whole breast irradiation. Patients needing lymph node treatment were not included. Additionally, no consideration was taken of breast size. A subsequent study could examine the effect of breast size on the radiation dose to LAD and LV for each of the five radiotherapy techniques used in this work. The female patients could be divided in different categories on the basis of the target volume. Further research is required to evaluate whether previously reported cardioprotective strategies [41] related to prone positioning, gating and proton therapy may have a considerable impact on LAD and LV exposure. It should also be mentioned that a follow-up study of patients irradiated for left-sided breast cancer, including the appropriate heart examinations, could reveal the association of radiation-induced cardiac complications with the dose absorbed by the LAD or LV.

## 5. Conclusions

A total of 115 radiotherapy plans were generated for left-sided breast cancer patients using 3D-CRT, 2F-IMRT, 7F-IMRT, VMAT1 and VMAT2. All the treatment plans were deemed clinically acceptable. Comparing the five irradiation techniques, the 7F-IMRT, VMAT1 and VMAT2 techniques proved to significantly reduce the  $V_{40Gy}$  and  $V_{30Gy}$  of the LAD and the  $V_{23Gy}$  of the LV. In contrast, the use of 3D-CRT was significantly superior in low-dose volume ( $V_{5Gy}$ ) for LV compared with other techniques. In conclusion, this research provides information for the LAD and LV radiation burden regarding the different treatment techniques with different beams and arc arrangements.

**Author Contributions:** Conceptualization, M.M.; methodology, M.M. and E.K.; software, E.K., A.V. and C.A.; validation, G.S. and M.M.; formal analysis, M.T.; investigation, M.M., E.K. and A.V.; resources, A.V.; writing—original draft preparation, E.K.; writing—review and editing, M.M. and M.T.; visualization, A.V., C.A. and M.T.; supervision, M.M.; project administration, M.M. All authors have read and agreed to the published version of the manuscript.

**Funding:** This research received no external funding.

**Institutional Review Board Statement:** The study was conducted in accordance with the Declaration of Helsinki and approved by the ethics committee of the University General Hospital of Heraklion, Crete, Greece (Reference: 4324/24-2-2023).

**Informed Consent Statement:** The requirement for informed consent was waived in this retrospective study.

**Data Availability Statement:** Data of this study are available from the corresponding author upon request.

**Conflicts of Interest:** The authors declare no conflicts of interest.

## References

1. Sung, H.; Ferlay, J.; Siegel, R.L.; Laversanne, M.; Soerjomataram, I.; Jemal, A.; Bray, F. Global Cancer Statistics 2020: GLOBOCAN Estimates of Incidence and Mortality Worldwide for 36 Cancers in 185 Countries. *CA Cancer J. Clin.* **2021**, *71*, 209–249. [\[CrossRef\]](#) [\[PubMed\]](#)
2. Howlader, N.; Noone, A.M.; Krapcho, M.; Miller, D.; Brest, A.; Yu, M.; Ruhl, J.; Tatalovich, Z.; Mariotto, A.; Lewis, D.R.; et al. (Eds.) *SEER Cancer Statistics Review, 1975–2018*; National Cancer Institute: Bethesda, MD, USA, 2023. Available online: [https://seer.cancer.gov/csr/1975\\_2018/](https://seer.cancer.gov/csr/1975_2018/) (accessed on 15 October 2023).
3. Duffy, S.W.; Tabár, L.; Yen, A.M.; Dean, P.B.; Smith, R.A.; Jonsson, H.; Törnberg, S.; Chen, S.L.; Chiu, S.Y.; Fann, J.C.; et al. Mammography Screening Reduces Rates of Advanced and Fatal Breast Cancers: Results in 549,091 Women. *Cancer* **2020**, *126*, 2971–2979. [\[CrossRef\]](#) [\[PubMed\]](#)
4. Kerr, A.J.; Dodwell, D.; McGale, P.; Holt, F.; Duane, F.; Mannu, G.; Darby, S.C.; Taylor, C.W. Adjuvant and Neoadjuvant Breast Cancer Treatments: A Systematic Review of Their Effects on Mortality. *Cancer Treat. Rev.* **2022**, *105*, 102375. [\[CrossRef\]](#) [\[PubMed\]](#)
5. Bellon, J.R.; Wong, J.S.; MacDonald, S.M.; Ho, A.Y. (Eds.) *Radiation Therapy Techniques and Treatment Planning for Breast Cancer*; Springer International Publishing: Cham, Switzerland, 2016. [\[CrossRef\]](#)
6. Early Breast Cancer Trialists' Collaborative Group. Effect of Radiotherapy after Breast-Conserving Surgery on 10-Year Recurrence and 15-Year Breast Cancer Death: Meta-Analysis of Individual Patient Data for 10 801 Women in 17 Randomised Trials. *Lancet* **2011**, *378*, 1707–1716. [\[CrossRef\]](#) [\[PubMed\]](#)
7. Early Breast Cancer Trialists' Collaborative Group. Effects of Radiotherapy and of Differences in the Extent of Surgery for Early Breast Cancer on Local Recurrence and 15-Year Survival: An Overview of the Randomised Trials. *Lancet* **2005**, *366*, 2087–2106. [\[CrossRef\]](#) [\[PubMed\]](#)
8. Darby, S.C.; Ewertz, M.; McGale, P.; Bennet, A.M.; Blom-Goldman, U.; Brønnum, D.; Correa, C.; Cutter, D.; Gagliardi, G.; Gigante, B.; et al. Risk of Ischemic Heart Disease in Women after Radiotherapy for Breast Cancer. *N. Engl. J. Med.* **2013**, *368*, 987–998. [\[CrossRef\]](#) [\[PubMed\]](#)
9. Cheng, Y.; Nie, X.; Ji, C.; Lin, X.; Liu, L.; Chen, X.; Yao, H.; Wu, S. Long-Term Cardiovascular Risk After Radiotherapy in Women With Breast Cancer. *J. Am. Heart Assoc.* **2017**, *6*, e005633. [\[CrossRef\]](#) [\[PubMed\]](#)
10. Wennstig, A.-K.; Wadsten, C.; Garmo, H.; Fredriksson, I.; Blomqvist, C.; Holmberg, L.; Nilsson, G.; Sund, M. Long-Term Risk of Ischemic Heart Disease after Adjuvant Radiotherapy in Breast Cancer: Results from a Large Population-Based Cohort. *Breast Cancer Res.* **2020**, *22*, 10. [\[CrossRef\]](#)
11. Correa, C.R.; Litt, H.I.; Hwang, W.-T.; Ferrari, V.A.; Solin, L.J.; Harris, E.E. Coronary Artery Findings After Left-Sided Compared With Right-Sided Radiation Treatment for Early-Stage Breast Cancer. *J. Clin. Oncol.* **2007**, *25*, 3031–3037. [\[CrossRef\]](#)
12. Sardar, P.; Kundu, A.; Chatterjee, S.; Nohria, A.; Nairouz, R.; Bangalore, S.; Mukherjee, D.; Aronow, W.S.; Lavie, C.J. Long-term Cardiovascular Mortality after Radiotherapy for Breast Cancer: A Systematic Review and Meta-analysis. *Clin. Cardiol.* **2017**, *40*, 73–81. [\[CrossRef\]](#)
13. Bouillon, K.; Haddy, N.; Delalogue, S.; Garbay, J.-R.; Garsi, J.-P.; Brindel, P.; Mousannif, A.; Lê, M.G.; Labbe, M.; Arriagada, R.; et al. Long-Term Cardiovascular Mortality after Radiotherapy for Breast Cancer. *J. Am. Coll. Cardiol.* **2011**, *57*, 445–452. [\[CrossRef\]](#) [\[PubMed\]](#)
14. Nilsson, G.; Holmberg, L.; Garmo, H.; Duvernoy, O.; Sjögren, I.; Lagerqvist, B.; Blomqvist, C. Distribution of Coronary Artery Stenosis After Radiation for Breast Cancer. *J. Clin. Oncol.* **2012**, *30*, 380–386. [\[CrossRef\]](#) [\[PubMed\]](#)
15. Wennstig, A.-K.; Garmo, H.; Isacson, U.; Gagliardi, G.; Rintelä, N.; Lagerqvist, B.; Holmberg, L.; Blomqvist, C.; Sund, M.; Nilsson, G. The Relationship between Radiation Doses to Coronary Arteries and Location of Coronary Stenosis Requiring Intervention in Breast Cancer Survivors. *Radiat. Oncol.* **2019**, *14*, 40. [\[CrossRef\]](#) [\[PubMed\]](#)
16. Jacob, S.; Camilleri, J.; Derreumaux, S.; Walker, V.; Lairez, O.; Lapeyre, M.; Bruguère, E.; Pathak, A.; Bernier, M.-O.; Laurier, D.; et al. Is Mean Heart Dose a Relevant Surrogate Parameter of Left Ventricle and Coronary Arteries Exposure during Breast Cancer Radiotherapy: A Dosimetric Evaluation Based on Individually-Determined Radiation Dose (BACCARAT Study). *Radiat. Oncol.* **2019**, *14*, 29. [\[CrossRef\]](#) [\[PubMed\]](#)
17. Kaidar-Person, O.; Zagar, T.M.; Oldan, J.D.; Matney, J.; Jones, E.L.; Das, S.; Jensen, B.C.; Zellars, R.C.; Wong, T.Z.; Marks, L.B. Early Cardiac Perfusion Defects after Left-Sided Radiation Therapy for Breast Cancer: Is There a Volume Response? *Breast Cancer Res. Treat.* **2017**, *164*, 253–262. [\[CrossRef\]](#) [\[PubMed\]](#)
18. Walker, V.; Lairez, O.; Fondard, O.; Pathak, A.; Pinel, B.; Chevelle, C.; Franck, D.; Jimenez, G.; Camilleri, J.; Panh, L.; et al. Early Detection of Subclinical Left Ventricular Dysfunction after Breast Cancer Radiation Therapy Using Speckle-Tracking Echocardiography: Association between Cardiac Exposure and Longitudinal Strain Reduction (BACCARAT Study). *Radiat. Oncol.* **2019**, *14*, 204. [\[CrossRef\]](#)
19. Fourati, N.; Charfeddine, S.; Chaffai, I.; Dhoubi, F.; Farhat, L.; Boukhris, M.; Abid, L.; Kammoun, S.; Mnejja, W.; Daoud, J. Subclinical Left Ventricle Impairment Following Breast Cancer Radiotherapy: Is There an Association between Segmental Doses and Segmental Strain Dysfunction? *Int. J. Cardiol.* **2021**, *345*, 130–136. [\[CrossRef\]](#)
20. Song, J.; Tang, T.; Caudrelier, J.-M.; Bélec, J.; Chan, J.; Lacasse, P.; Aldosary, G.; Nair, V. Dose-Sparing Effect of Deep Inspiration Breath Hold Technique on Coronary Artery and Left Ventricle Segments in Treatment of Breast Cancer. *Radiother. Oncol.* **2021**, *154*, 101–109. [\[CrossRef\]](#)

21. Eber, J.; Schmitt, M.; Dehaynin, N.; Le Fèvre, C.; Antoni, D.; Noël, G. Evaluation of Cardiac Substructures Exposure of DIBH-3DCRT, FB-HT, and FB-3DCRT in Hypofractionated Radiotherapy for Left-Sided Breast Cancer after Breast-Conserving Surgery: An In Silico Planning Study. *Cancers* **2023**, *15*, 3406. [\[CrossRef\]](#)
22. Chang, J.S.; Chang, J.H.; Kim, N.; Kim, Y.B.; Shin, K.H.; Kim, K. Intensity Modulated Radiotherapy and Volumetric Modulated Arc Therapy in the Treatment of Breast Cancer: An Updated Review. *J. Breast Cancer* **2022**, *25*, 349. [\[CrossRef\]](#)
23. Kuzba-Kryszak, T.; Nowakowski, S.; Winiecki, J.; Makarewicz, R. Comparative Analysis of the Absorbed Dose in the Heart and Anterior Descending Branch of the Left Coronary Artery (LAD) in Patients with Left-Sided Breast Cancer Who Received Radiotherapy Using 3D-CRT, IMRT and VMAT Techniques. *J. BUON Off. J. Balk. Union Oncol.* **2021**, *26*, 753–758.
24. Offersen, B.V.; Boersma, L.J.; Kirkove, C.; Hol, S.; Aznar, M.C.; Biete Sola, A.; Kirova, Y.M.; Pignol, J.-P.; Remouchamps, V.; Verhoeven, K.; et al. ESTRO Consensus Guideline on Target Volume Delineation for Elective Radiation Therapy of Early Stage Breast Cancer. *Radiother. Oncol.* **2015**, *114*, 3–10. [\[CrossRef\]](#) [\[PubMed\]](#)
25. Duane, F.; Aznar, M.C.; Bartlett, F.; Cutter, D.J.; Darby, S.C.; Jagsi, R.; Lorenzen, E.L.; McArdle, O.; McGale, P.; Myerson, S.; et al. A Cardiac Contouring Atlas for Radiotherapy. *Radiother. Oncol.* **2017**, *122*, 416–422. [\[CrossRef\]](#) [\[PubMed\]](#)
26. Biedka, M.; Zmuda, E. Contouring of the left anterior descending coronary artery in patients with breast cancer—The radiation oncologist's view. *Nowotowory. J. Oncol.* **2020**, *70*, 60–64.
27. Goyal, S.; Buchholz, T.; Haffy, G.B. Breast Cancer: Early Stage. In *Principles and Practice of Radiation Oncology*, 7th ed.; Halperin, C.E., Wazer, E.D., Perez, A.C., Brady, W.L., Eds.; Wolters Kluwer: Philadelphia, PA, USA, 2019; p. 1332.
28. Jeulink, M.; Dahele, M.; Meijnen, P.; Slotman, B.J.; Verbakel, W.F.A.R. Is There a Preferred IMRT Technique for Left-breast Irradiation? *J. Appl. Clin. Med. Phys.* **2015**, *16*, 197–205. [\[CrossRef\]](#) [\[PubMed\]](#)
29. Kataria, T.; Goyal, S.; Malik, A.; Kumar, K.; Shyam, S.B.; Deepak, G. Modulated Radiotherapy for Breast Cancer: Locoregional Outcomes. *Int. J. Radiol. Radiat. Ther.* **2016**, *1*, 00003. [\[CrossRef\]](#)
30. Thomsen, M.S.; Berg, M.; Zimmermann, S.; Lutz, C.M.; Makocki, S.; Jensen, I.; Hjelstuen, M.H.B.; Pensold, S.; Hasler, M.P.; Jensen, M.-B.; et al. Dose Constraints for Whole Breast Radiation Therapy Based on the Quality Assessment of Treatment Plans in the Randomised Danish Breast Cancer Group (DBCG) HYPO Trial. *Clin. Transl. Radiat. Oncol.* **2021**, *28*, 118–123. [\[CrossRef\]](#) [\[PubMed\]](#)
31. Piroth, M.D.; Baumann, R.; Budach, W.; Dunst, J.; Feyer, P.; Fietkau, R.; Haase, W.; Harms, W.; Hehr, T.; Krug, D.; et al. Heart Toxicity from Breast Cancer Radiotherapy: Current Findings, Assessment, and Prevention. *Strahlenther. Onkol.* **2019**, *195*, 1–12. [\[CrossRef\]](#)
32. Chen, C.-P.; Chen, T.-H.; Chiou, J.-F.; Chen, Y.-J.; Kuo, C.-C.; Tseng, K.-H.; Chung, M.-Y.; Chen, C.-Y.; Wu, J.-Y.; Lu, L.-S.; et al. Retrospective Analysis for Dose Reduction to Organs at Risk with New Personalized Breast Holder (PERSBRA) in Left Breast IMRT. *J. Pers. Med.* **2022**, *12*, 1368. [\[CrossRef\]](#)
33. Ott, O.J.; Stillkrieger, W.; Lambrecht, U.; Schweizer, C.; Lamrani, A.; Sauer, T.-O.; Strnad, V.; Bert, C.; Hack, C.C.; Beckmann, M.W.; et al. External-Beam-Accelerated Partial-Breast Irradiation Reduces Organ-at-Risk Doses Compared to Whole-Breast Irradiation after Breast-Conserving Surgery. *Cancers* **2023**, *15*, 3128. [\[CrossRef\]](#)
34. Ratosa, I.; Jenko, A.; Sljivic, Z.; Pirnat, M.; Oblak, I. Breast Size and Dose to Cardiac Substructures in Adjuvant Three-Dimensional Conformal Radiotherapy Compared to Tangential Intensity Modulated Radiotherapy. *Radiol. Oncol.* **2020**, *54*, 470–479. [\[CrossRef\]](#) [\[PubMed\]](#)
35. Mazonakis, M.; Kachris, S.; Tolia, M.; Damilakis, J. NTCP Calculations of Five Different Irradiation Techniques for the Treatment of Thymoma. *Curr. Oncol.* **2023**, *30*, 7740–7752. [\[CrossRef\]](#) [\[PubMed\]](#)
36. Matsali, E.; Pappas, E.P.; Lyraraki, E.; Lymperopoulou, G.; Mazonakis, M.; Karaikos, P. Assessment of Radiation-Induced Bladder and Bowel Cancer Risks after Conventionally and Hypo-Fractionated Radiotherapy for the Preoperative Management of Rectal Carcinoma. *J. Pers. Med.* **2022**, *12*, 1442. [\[CrossRef\]](#) [\[PubMed\]](#)
37. Lin, Y.-H.; Cheng, J.-Y.; Huang, B.-S.; Luo, S.-D.; Lin, W.-C.; Chou, S.-Y.; Juang, P.-J.; Li, S.-H.; Huang, E.-Y.; Wang, Y.-M. Significant Reduction in Vertebral Artery Dose by Intensity Modulated Proton Therapy: A Pilot Study for Nasopharyngeal Carcinoma. *J. Pers. Med.* **2021**, *11*, 822. [\[CrossRef\]](#) [\[PubMed\]](#)
38. Rezaeij, S.M.; Hashemi, B.; Mofid, B.; Bakhshandeh, M.; Mahdavi, A.; Hashemi, M.S. The Feasibility of a Dose Painting Procedure to Treat Prostate Cancer Based on mpMR Images and Hierarchical Clustering. *Radiat. Oncol.* **2021**, *16*, 182. [\[CrossRef\]](#) [\[PubMed\]](#)
39. Zhang, L.; Mei, X.; Chen, X.; Hu, W.; Hu, S.; Zhang, Y.; Shao, Z.; Guo, X.; Tuan, J.; Yu, X. Estimating Cardiac Substructures Exposure From Diverse Radiotherapy Techniques in Treating Left-Sided Breast Cancer. *Medicine* **2015**, *94*, e847. [\[CrossRef\]](#)
40. Karpf, D.; Sakka, M.; Metzger, M.; Grabenbauer, G.G. Left Breast Irradiation with Tangential Intensity Modulated Radiotherapy (t-IMRT) versus Tangential Volumetric Modulated Arc Therapy (t-VMAT): Trade-Offs between Secondary Cancer Induction Risk and Optimal Target Coverage. *Radiat. Oncol.* **2019**, *14*, 156. [\[CrossRef\]](#)
41. Nikovia, V.; Chinis, E.; Gkantaifi, A.; Marketou, M.; Mazonakis, M.; Charalampakis, N.; Mavroudis, D.; Orfanidou, K.V.; Varveris, A.; Antoniadis, C.; et al. Current Cardioprotective Strategies for the Prevention of Radiation-Induced Cardiotoxicity in Left-Sided Breast Cancer Patients. *J. Pers. Med.* **2023**, *13*, 1038. [\[CrossRef\]](#)

**Disclaimer/Publisher's Note:** The statements, opinions and data contained in all publications are solely those of the individual author(s) and contributor(s) and not of MDPI and/or the editor(s). MDPI and/or the editor(s) disclaim responsibility for any injury to people or property resulting from any ideas, methods, instructions or products referred to in the content.